Crystal-field model study of the xenon hexafluoride molecule. II. Comparisons with other hexavalent xenon molecules

Sylvester Y. Wang and Lawrence L. Lohr, Jr.

Department of Chemistry, University of Michigan, Ann Arbor, Michigan 48104
(Received 25 June 1973)

The two-electron crystal-field model previously used to describe in detail the energy levels of XeF_6 is applied to other hexavalent xenon systems, namely the $XeOF_4$, XeO_2F_2, and XeO_3 molecules and the XeF_8^{2-} ion. Comparisons of the calculated excited state energies of these three molecules at their observed geometries are made to those calculated for various geometries of XeF_6. The strong low symmetry fields in $XeOF_4$, XeO_2F_2, and XeO_3 result in very high excitation energies, which may also be taken to represent greater energy stabilization for the lone electron pair relative to that for XeF_6. The ground state energy of XeF_8^{2-} is explored as a function of geometry, and within the two-space considered, the results match the structure observed in solid $(NO)_2XeF_8$.

I. INTRODUCTION

In a recent publication[1] we have outlined in detail a two-electron crystal-field model of the electronic structure of the XeF_6 molecule and presented results for the ground and excited state energies as a function of molecular geometry and of several energy parameters. It is the purpose of this paper to put the XeF_6 results into chemical perspective by comparisons with the results of similar calculations on other Xe (VI) systems, each described in terms of the wavefunctions for the highest energy electron pair in an effective "crystal field" generated by the nuclei and the rest of the electrons in the molecule. The computational details[1] are not repeated here, except to point out that the energies and wavefunctions are obtained by the diagonalization of a 28×28 matrix representing crystal-field, electron-repulsion, and spin–orbit interactions within the basis of the 28 two-electron states constructed from xenon 5s and 5p orbitals. Ligand–ligand interactions are also included via point-charge repulsions and make an important contribution to the shapes of potential energy curves. The necessary parameters[1] are the effective one-electron energy gap ΔE_{5s-5p}, the electron-repulsion integrals F_1 (5s, 5p) and F_2 (5p, 5p), the one-electron spin–orbit parameter ζ_{5p}, and the radial integrals $\langle r^2 \rangle_{pp}^{1/2}$ and $\langle r \rangle_{sp}$. The four energy parameters are taken in this study to be the same as those used in most of the XeF_6 calculations, and are given in Sec. II. The radial integral $\langle r^2 \rangle_{pp}^{1/2}$ is the root-mean-square electron radius for the 5p orbital, while $\langle r \rangle_{sp}$ is the radial matrix element of scalar r between 5s and 5p. The values of these parameters are the same as those used before, namely 1.64954 and 2.05495 a.u., respectively.

II. THE $XeOF_4$, XeO_2F_2, AND XeO_3 MOLECULES

In this section we present results of crystal-field calculations of the type previously described, but here applied to molecules other than XeF_6. The energy parameters were kept at the values $\Delta E_{5s-5p} = 3.5$ eV, $F_1 = 0.5$ eV, $F_2 = 0.08$ eV, and $\zeta_{5p} = 0.87$ eV, these values corresponding to the so-called "best" set of those used in the XeF_6 study.[1] For each of the molecules $XeOF_4$, XeO_2F_2, and XeO_3, only a single geometry was considered, with that being a reported equilibrium geometry. Charges of -2 for oxygen and -1 for fluorine

were used in the crystal-field analysis. The microwave structure[2] of $XeOF_4$ is characterized by C_{4v} symmetry and bond lengths of 1.70 ± 0.05 Å for Xe–O and 1.95 ± 0.05 Å for Xe–F, with an $\angle$O–Xe–F of $91° \pm 2°$. The structural parameters we used were 1.71 Å for Xe–O and 1.90 Å for Xe–F (this latter value chosen to be essentially the same as that for XeF_6), with an $\angle$O–Xe–F of $90°$, implying that the four fluorines are coplanar with the xenon atom. These bond lengths are in fact the refined microwave values as quoted[3] by Begun, Fletcher, and Smith, based on a private communication from Martins and Wilson. For XeO_2F_2 we assumed a C_{2v} structure, as indicated[4] by its vibrational spectra, with assumed parameters of 1.90 Å for Xe–F, 1.70 Å for Xe–O, $\angle$O–Xe–O = $100°$ and $\angle$O–Xe–F = $90°$, thus making the structure much like that determined[5] by x rays for the isoelectronic $IO_2F_2^-$ ion in the solid KIO_2F_2. Finally the C_{3v} structure for XeO_3 is taken to be that determined[6] by x rays for the solid, with 1.76 Å for Xe–O and $\angle$O–Xe–O = $103°$.

The crystal-field results for the $XeOF_4$ and XeO_3 molecules are shown in Fig. 1, together with those for three different structures of XeF_6, namely octahedral, C_{3v} (at radial minimum[1] in pure t_{1u} bending space), and C_{3v} (at minimum[1] in $t_{1u}-t_{2g}$ bending space). For comparative purposes the energy of the lowest two-electron state [$^1S_0$ of free Xe(+6) ion] is assigned a value of zero for each species, with the shaded regions grouping together all levels associated with the same orbital configuration. Structure within each shaded region is indicated by horizontal lines and results from exchange splittings and spin–orbit coupling. Thus, for XeF_6 (O_h), there are three groupings corresponding to the configurations $5s^2$, $5s5p$, and $5p^2$, while for $XeOF_4$ and XeO_3, with strong axial fields, there are six groupings. For the distorted XeF_6 structures some of these groupings are incompletely separated, so that four are shown. The ground-state stabilization of XeF_6 accompanying t_{1u} deformations is reflected in Fig. 1 as an *increase* in the excitation energies relative to those of the O_h structure. The excited states are even higher in energy for $XeOF_4$ and XeO_3, where the large axial fields not only mix 5s and 5p orbitals to a considerable degree but also split the 5p orbitals by a very large first-order effect from the $l=2$ part of the field. Indeed the first absorp-

TABLE I. Comparison of energy levels.[a,b].

Level	$\lvert M_J\rvert$	$XeF_6(O_h)$	XeOF$_4$	XeO$_3$
$^1S_0$	0	0.0	0.0	0.0
$^3P_0^0$	0	2.48	7.24	7.19
$^3P_1^0$	0	2.68	7.22	7.18
	1	2.68	7.65	7.60
$^3P_2^0$	0	3.78	11.88	14.86
	1	3.78	11.90	14.85
	2	3.78	8.14	8.08
$^1P_1^0$	0	4.58	11.87	14.83
	1	4.58	8.48	8.46
$^3P_0$	0	5.44	15.73	15.65
$^3P_1$	0	6.42	20.16	22.91
	1	6.42	16.28	16.15
$^3P_2^i$	0	6.70	17.78	17.65
	1	6.70	20.47	23.34
	2	6.70	16.75	23.80
$^1D_2$	0	7.93	20.03	23.01
	1	7.93	21.20	24.07
	2	7.93	20.94	16.63
$^1S_0$	0	8.70	25.66	31.55

[a] All energies are in electron volts and relative to that for the lowest level for each species. The energy parameters are $\Delta E_{5s-5p} = 3.5$ eV, $F_1 = 0.5$ eV, $F_2 = 0.08$ eV, and $\zeta_{5p} = 0.87$ eV.
[b] Molecular levels are designated by the principal free-ion level, as ascertained by inspection of the eigenvectors in a free-ion basis. For XeOF$_4$ (C_{4v}) and XeO$_3$ (C_{3v}), only M_J is a "good" quantum number; specifically L, S, J, and the parity are not.

tion bands for XeOF$_4$ and XeO$_3$ are predicted to occur at almost twice the energy of those for XeF$_6$ $(C_{3v}$, combined t_{1u} and t_{2g} distortions), with both spin singlet and triplet states contained within the shaded region for the $5s5p_x$ and $5s5p_y$ configurations (the molecular symmetry axis is taken to be z). The energies are given in detail in Table I, where the levels are designated by the principal free-ion Xe(+6) level. All levels with $\lvert M_J\rvert > 0$ are doubly denerate, with M_J being the only "good" quantum number for the axially symmetric molecules. The liquid state of XeOF$_4$ is described[7] as colorless, with a refractive index $n_D = 1.4215$ at 25 °C, while XeO$_3$ is a white solid. The low value of n_D certainly argues against the presence of low-lying electronic states for XeOF$_4$. An interesting feature in Fig. 1 is that the energy difference between the $5s$ and the $5p_x$ or $5p_y$ orbitals is virtually the same for XeOF$_4$ and XeO$_3$, while the $5s-5p_z$ difference is significantly greater (about 25%) in XeO$_3$.

Although similar results were obtained for XeO$_2$F$_2$ (C_{2v}), these are not presented in detail here. The low symmetry causes the degeneracy of the spin–orbit levels to be completely lifted, while the levels themselves are not as well separated according to the various two-electron configurations. In general the XeO$_2$F$_2$ excitation energies are roughly 10% higher than the corresponding ones for XeO$_3$. Specifically the lowest triplet component is calculated to occur at 8.1 eV in

XeO$_2$F$_2$, as compared to 7.2 eV in XeO$_3$ and XeOF$_4$, 4.2 eV in XeF$_6$(C_{3v}, t_{1u} and t_{2g}), 3.2 eV in XeF$_6$ (C_{3v}, t_{1u} only), and 2.5 eV in XeF$_6$ (O_h). XeO$_2$F$_2$, like XeO$_3$, is a white solid, so that the results appear consistent, at least, even though an excitation energy of 65 000 cm^{-1} seems excessive.

It is interesting to compare these results with those from a recent[8] Wolfsberg–Helmholz (extended Hückel) treatment of XeOF$_4$, XeO$_2$F$_2$, and the T-shaped tetravalent species XeOF$_2$. These studies employed an F($2s$ and $2p$) and Xe ($5s$ and $5p$) basis in the semiempirical construction of molecular orbitals. For XeOF$_4$ the highest occupied MO is of a_1 symmetry in group C_{4v} and is a strongly admixed orbital containing Xe ($5s$), Xe($5p$), and F($2p\sigma$) orbitals. Its energy is 9.85 eV below the unoccupied (virtual) e orbital consisting largely of Xe($5p$), and 20.38 eV below the unoccupied and strongly antibonding a_1 orbital, the latter containing some O($2p\sigma$) character. For XeO$_2$F$_2$(C_{2v}) the gap between the highest occupied (a_1) orbital and the lowest unoccupied (b_1) orbital is 14.39 eV, much larger than for XeOF$_4$, a result qualitatively identical to our crystal-field conclusion concerning higher exictation energies in XeO$_2$F$_2$ than in XeOF$_4$. The Xe (IV) species XeOF$_2$ corresponds to a four-electron system in our method, and could be treated as such, although we have not done so. Here the gap between the highest occupied (a_1) and the lowest unoccupied (b_2) orbital is 15.28 eV, larger than for XeOF$_4$. Interestingly the extra lone pair [relative to Xe(VI) sys-
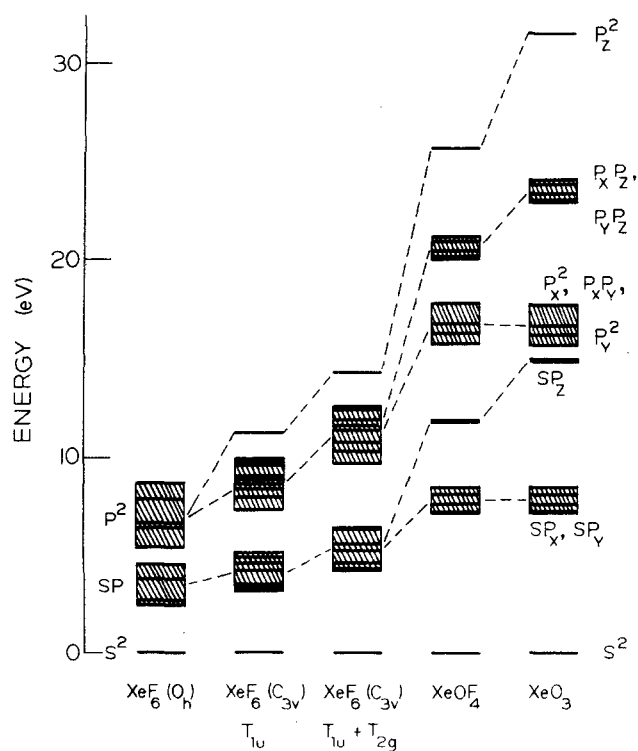

FIG. 1. Energy levels in electron volts for XeOF$_4(C_{4v})$ and XeO$_3$ (C_{3v}) compared to those for three different structures of XeF$_6$ (see Ref. 1). Electronic parameters are $\Delta E_{5s-5p} = 3.5$ eV, $F_1 = 0.5$ eV, $F_2 = 0.08$ eV, and $\zeta_{5p} = 0.87$ eV. Horizontal lines denote each energy, but the double degeneracy of some levels is not indicated. Shaded areas enclose all levels of a given two-electron configuration. See Table I for detailed values.

tems] is in a b_1 orbital with an energy 1.3 eV *below* that of the a_1 orbital. The number and arrangement of the ligands permits a low energy for an extra pair, as it does for square-planar XeF_4.

For all species considered in this section, the high electronic excitation energies as compared to those computed for XeF_6, O_h or C_{3v}, can be taken to reflect an enhanced energy stabilization of the two-electron ground state, which is often referred to as the "lone pair." The semiempirical molecular orbital results[8] can be given a similar interpretation, with the strong low-symmetry fields producing greater $5s$–$5p$ mixing than even in distorted XeF_6.

III. XeF_8^{2-} ION

A species closely related to XeF_6 is the XeF_8^{2-} anion, such as present in the crystalline solid $(NO)_2XeF_8$, nitrosonium octafluoroxenate (VI). The x-ray studies[9] of this material reveal a slightly distorted Archimedian antiprismatic structure for XeF_8^{2-}. Although only a mirror plane symmetry for the ion is required by the orthorhombic space group *Pnma*, the structure is close to the D_{4d} symmetry of an antiprism. The five different Xe–F bond lengths are found to be 1.946(5), 1.958(7), 1.971(7), 2.052(5), and 2.099(5) Å. The average polar angle for the ligands with respect to the approximate S_8 axis is 57.9° (or 180° − 57.9° = 122.1°).

We have carried out crystal-field calculations similar to those for the other Xe(+6) systems, using the same energy parameters and an Xe–F distance of 2.0 Å, close to the observed average. Specifically we have explored the variation of the ground-state energy, including ligand–ligand repulsions, as a function of the two angles necessary for describing a complex of assumed D_4 symmetry. These angles are a polar angle θ and an azimuthal angle ϕ, where $\phi = 0$, 90°, 180°, or 270° for D_{4h} structures, and $\phi = 45°$, 135°, 225°, or 315° for D_{4d} structures. The resulting potential energy contours are shown in Fig. 2. The minimum energy occurs for a D_{4d} structure ($\phi = 45°$) with $\theta = 57°$, essentially identical to the observed average of 57.9° (the observed angle ranges from 56.1° to 58.7° for various fluorines in the C_s complex). This D_{4d} structure is flattened with respect to a "rotated" cube for which $\theta = \cos^{-1}(3^{-1/2}) = 54.74°$, but not so flattened as a D_{4d} polyhedron with two square and eight equilateral triangular faces for which $\theta = \tan^{-1}(8^{-1/4}) = 59.26°$ (the true antiprism). The energy at the D_{4d} minimum in the two space of Fig. 2 is 0.54 eV below that for a cubal O_h structure. Our results are largely due to ligand repulsions, as there is no $5s$–$5p$ mixing for the general symmetry D_4 of this surface. A consequence of this is the further result that energy differences between ground and excited states are, in our model, essentially the same, except for small splittings due to the $l = 2$ part of the crystal field, as those for XeF_6 (O_h). It should be pointed out that we have not considered geometries for XeF_8^{2-} which would permit significant $5s$–$5p$ mixing and thus provide a ninth coordination position for the lone pair. Throughout our surface (Fig. 2), the lone pair remains in a spherical $5s^2$ distribution (there is of course some mixing with the

$^1S_0$ and $^3P_0$ levels of $5p^2$). It should also be noted that a cubal (O_h) structure for XeF_8^{2-} corresponds to a saddle point in Fig. 2, this structure being at a minimum with respect to the angle θ, but a maximum with respect to the angle ϕ.

There are other Xe(VI) systems which we have not considered as very little is known about them at this time. These include the ion XeF_5^+, present[10] in $XeF_6 \cdot BF_3$ and possibly[11,12] in other adducts, such as those with SbF_5, SnF_4, GeF_4, etc.; the ion XeF_7^- which *may* be present[13] in the solids $CsXeF_7$ and $RbXeF_7$; and the ion XeO_4^{-2}, present[14] in the solid xenate $CsHXeO_4$. With respect to the latter species, our model would yield for an XeO_4^{2-} species with assumed tetrahedral symmetry identical energy levels to those for $XeF_6(O_h)$, provided that identical energy parameters were used in the two cases. These parameters differ, of course, rather considerably from those for an isolated Xe (+6) ion due to nephelauxetic and related effects, and perhaps should be significantly lower for XeO_4^{2-} as compared to XeF_6. The pseudo-Jahn–Teller active modes for XeO_4^{2-} would, of course, be the t_2 bending and stretching modes, which would mix $5s$ and $5p$ xenon orbitals.

There remains the important problem of the ultraviolet absorption spectrum of gaseous XeF_6. A significant feature of the reported[15] spectrum is the long "tail" of the first absorption band at approximately 3400 Å (29 400 cm^{-1}), with this tail not only extending well into the visible (to about 4500 Å), but also showing a marked
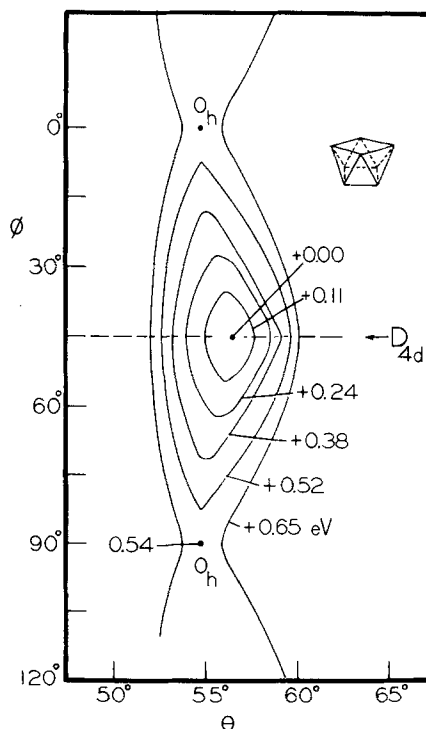

FIG. 2. Potential energy contours in electron volts for the ground state of XeF_8^{2-} with Xe–F = 2.0 Å and electronic parameters $\Delta E_{5s-5p} = 3.5$ eV, $F_1 = 0.5$ eV, $F_2 = 0.08$ eV, and $\zeta_{5p} = 0.87$ eV. The molecular symmetry is at least D_4 at all points on this surface, with cubal O_h structures occurring when the azimuthal angle ϕ is 0° or 90° and the polar angle $\theta = 54.74°$. Structures with $\phi = 45°$ have D_{4d} symmetry.

increase in absorbance upon increasing the sample temperature from 25 to 90 °C. By contrast the absorbance decreases with increasing temperature in the spectral range 3000–3300 Å. These and other spectral features were interpreted[16] within the framework of an electronic isomers model, in which the XeF_6 vapor is described as an equilibrium mixture of octahedral spin–singlet ground-state molecules and trigonally distorted (both prolate and oblate), spin–triplet excited state molecules. Part III of this series will present the spectral energies, intensities, and band shapes as obtained from our two-electron crystal-field model.

[1]S. W. Wang and L. L. Lohr, Jr., J. Chem. Phys. 60, 3901 (1974), the preceding article.

[2]J. Martins and E. B. Wilson, J. Chem. Phys. 41, 570 (1964).

[3]G. M. Begun, W. H. Fletcher, and D. F. Smith, J. Chem. Phys. 42, 2236 (1965).

[4]H. H. Claassen, E. L. Gasner, H. Y. Kim, and J. L. Huston, J. Chem. Phys. 49, 253 (1968).

[5]L. Helmholz and M. T. Rogers, J. Am. Chem. Soc. 62, 1537 (1940).

[6]D. H. Templeton, A. Zalkin, and J. D. Forrester, J. Am. Chem. Soc. 85, 817 (1963).

[7]H. H. Hyman, in *Physical Chemistry: An Advanced Treatise*, edited by (H. Eyring, D. Henderson, and W. Jost (Academic, New York, 1970), Vol. 5, pp. 589–662.

[8]S.-C. Hsu, C.-Y Ng, and W.-K. Li, J. Mol. Struct. 16, 125 (1973).

[9]S. W. Peterson, J. H. Holloway, B. A. Coyle, and J. M. Williams, Science 173, 1238 (1971); the preparation of $(NO)_2XeF_8$ is reported by G. J. Moody and H. Selig, Inorg. Nucl. Chem. Lett. 2, 319 (1966).

[10]H. Selig, Science 144, 537 (1964).

[11]G. L. Gard and G. H. Cady, Inorg. Chem. 3, 1745 (1964).

[12]K. E. Pullen and G. H. Cady, Inorg. Chem. 5, 2057 (1966); 6, 1300 (1967).

[13]R. D. Peacock, H. Selig, and I. Sheft, Proc. Chem. Soc. 1964, 285.

[14]B. Jaselkis, T. M. Spittler, and J. L. Huston, J. Am. Chem. Soc. 88, 2149 (1966).

[15]H. H. Claassen, G. L. Goodman, and H. Kim, J. Chem. Phys. 56, 5042 (1972).

[16]G. L. Goodman, J. Chem. Phys. 56, 5038 (1972).